Al_2O_3 and Fe_3O_4 Coated SMCs: Effect of Coating Material and Milling Time on Magnetic and Mechanical Properties

Katie Jo Sunday and Mitra L. Taheri
Drexel University
Philadelphia, PA 19104

Kristopher Darling
U.S. Army Research Laboratory
Aberdeen, MD 21005

Francis Hanejko
Hoeganaes Corporation
Cinnaminson, NJ 08077

ABSTRACT

Soft magnetic composites (SMCs) have 3D magnetic flux carrying capabilities, reduced core losses, reduced size and weight, and lower manufacturing time and cost. Not only will SMCs replace traditional lamination steel, but also they will transform electromagnetic applications indefinitely. Ferrous powders need proper electrical insulation in order to confine eddy currents within individual particles, by eliminating metal-on-metal contact points, which encourage eddy current flow. Mechanically milled iron powders are insulated with high temperature coating materials such as Al_2O_3 and Fe_3O_4, then compacted and cured under conventional powder metallurgy (PM) techniques, and analyzed for their magnetic, mechanical, and structural properties. Milling times and coating thicknesses are investigated to optimize magnetization saturation, coercivity, and hardness of powder compacts.

INTRODUCTION

The demand for more efficient and cost effective electromagnetic devices, such as electric motors and transformers, has been driven by the rising green automobile and aerospace industries [1, 2]. Alternatives to traditional silicon steel laminations are necessary to improve electrical, magnetic, and mechanical properties [3] and for use in higher frequency applications such as jet engines and electric motors [4–6]. Laminations restrict the flow of magnetic flux parallel to specific planes due to their geometries and cause large eddy current losses when not coated properly, both contributing to very low electrical efficiency [7]. One method to overcome these downfalls is to electrically insulate magnetic, metallic particles (iron-, nickel-, or cobalt-alloys), press them into the desired shape, and subsequently heat treat them to produce the most advantageous SMC [8– 12]. Compaction allows for maximum density to be achieved, which directly contributes to higher magnetic permeability by eliminating undesired air gaps; however, during compaction, powders experience further deformation resulting in higher coercivities and hysteresis losses due to increased mechanical strain and the formation of additional internal defects [13]. To partly relieve

these stresses, powder compacts are cured for extensive amounts of recovery, grain growth, and magnetic domain wall movement, which can improve magnetic properties. Iron-based SMCs should be cured above 700°C to remove internal defects in order to improve magnetic permeability [14]; however, this also jeopardizes the mechanical properties obtained by milling.

SMCs are comprised of ferromagnetic powders, completely isolated from one another via an electrical insulator, compacted and cured, so that metal-on-metal contact points are avoided. Powders themselves possess advantageous properties relevant to higher frequency applications. Powders permit three-dimensional magnetic flux carrying capabilities because their geometries are not limited in any one direction and allow for complex designs, unlike laminations. The strongest benefit of SMCs is that they eliminate eddy current losses by properly insulating every single particle. By doing so, the overall efficiency is greatly improved and less metallic material is required, therefore greatly reducing the overall size and weight of the device. Lastly, manufacturing time and cost are reduced due to fewer processing steps and less waste, by utilizing PM materials and methods. Potential insulators are organic materials such as epoxy resins or silicone polymers often deployed as binders and inorganic materials such as ceramics or oxides often utilized as coatings.

Dielectric, organic coatings typically have a maximum annealing temperature of 450°C before they begin to degrade, resulting in low mechanical strength and metal-on-metal contact points that lead to low magnetic permeability [15]. Such a temperature does not allow for regions of high stress to be relieved in iron, leading to hard magnetic properties. Therefore, a reasonable balance of interparticle insulation and iron content is necessary in order to obtain maximum performance. In addition, a strong balance between deformation, obtained through milling and compaction, and stress relief from curing temperatures is necessary to produce the best soft magnetic material for high frequency electromagnetic applications. High temperature coatings such as MgO, ZrO_2, Al_2O_3, and Fe_3O_4 are highly resistive and if properly utilized can completely insulate ferrous powders to reduce core losses [16–18]. These materials possess high melting temperatures, which allow them to remain stable at necessary stress relief temperatures of iron. Alumina (Al_2O_3) ceramic has a very high resistivity (10^{14} -10^{15} Ωm) and melting temperature (~2050°C); however, due to alumina's nonmagnetic nature, the overall magnetization will be reduced [19]. Magnetite (Fe_3O_4) on the other hand is ferrimagnetic (92 emu/g), which aids the magnetization of iron powders in an SMC [20]. Magnetite does have a lower melting temperature (~1600°C) and lower resistivity than alumina, therefore a proper balance can be found of each material separately or combined as electrically insulating coatings of iron powder SMCs.

METHODS

We have investigated the effect of two types of inorganic coatings on iron powders using x-ray diffraction (XRD), scanning electron microscopy (SEM) with energy dispersive x-ray spectroscopy (EDS), vibrating sample magnetometry (VSM), and nanoindentation. We utilized dry coating methods based on Van der Waals interactions between host (Fe) particles and guest (coating) material [21]. These forces allow for large powders to be completely coated with smaller particles based on the kinetic energy and amount of contact points that occur. Wet and dry chemistry methods have been employed for coating iron-alloy powders with protective layers to reduce eddy currents and improve electrical efficiency [18, 22, 23]. We utilized traditional milling techniques to develop a non-traditional coating method for sufficiently insulating metallic powders.

High purity iron powder with average particle sizes of 300 μm were coated with alumina and magnetite, both separately as well as subsequently combined. Mechanical milling was performed in a SPEX 8000M high-energy shaker mill with an alumina ceramic vial or a hardened steel (HS) metallic vial, supplied from SPEX SamplePrep [24]. Al_2O_3 media balls or hardened steel media balls of 2 mm diameters were utilized with ball-to-powder ratios of 1:1 (vol.%) during initial milling.

Manipulating one step of the experimental procedure produced three coating types, Al_2O_3, Al_2O_3/Fe_3O_4, and Fe_3O_4. Alumina coated iron powders were produced by milling Fe powder with Al_2O_3

media balls in an Al_2O_3 vial for 2 to 24 h, with no additional material added. The media balls were removed and the coated powder was uniaxially compacted in a tungsten carbide die of 3 mm diameter at 3 GPa pressure and subjected to curing temperatures of 500°C to 900°C for 1 h in an argon and hydrogen (3 %) atmosphere.

The double layer coating of alumina and magnetite was produced by utilizing hardened steel media balls in place of Al_2O_3 media balls and as seen in Figure 1. After the HS media balls were removed, Fe_3O_4 particles of 1 to 5 μm sizes were added and powders were milled for an additional hour. Iron powders coated solely with magnetite used hardened steel media balls with a hardened steel vial, removed media balls, added Fe_3O_4 particles, and milled for 1 h. Initial milled powders and coated powders were characterized by x-ray diffraction (XRD) with a Rigaku SmartLab diffractometer utilizing Cu-Kα radiation (λ =1.541 Å). Twelve hour θ - 2θ scans from 5° to 120° with a step size of 0.02° and speed of 7.5 (deg./min) were necessary for proper identification of elemental phases and microstrain caused by peak broadening effects. The Voigt function method [25] was used to determine crystallite size (Lorentzian fit) and microstrain (Gaussian fit) on milled powders for a single line analysis [26].

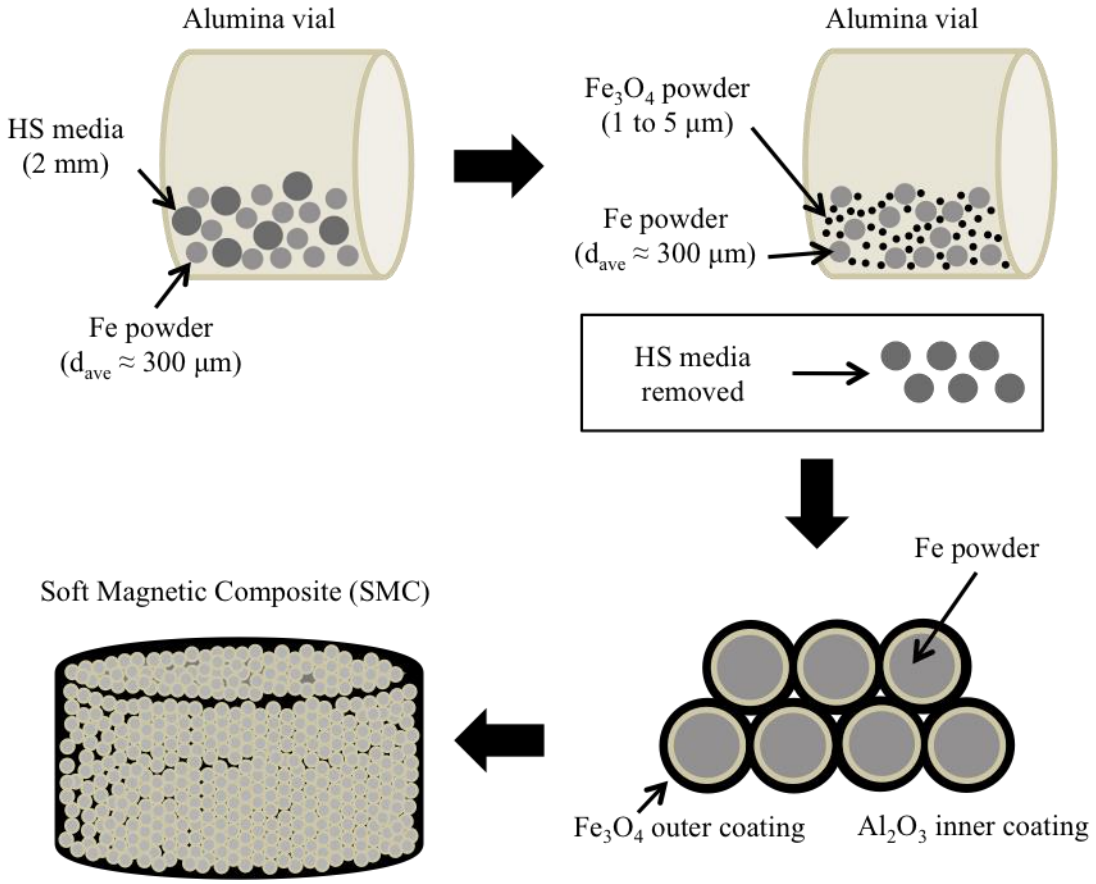

Figure 1. Procedure for the dual layer of alumina and magnetite coated iron powders.

Powder shapes and sizes as well as surface morphologies were examined using an FEI scanning electron microscope (SEM). Furthermore, SEM coupled with EDS allowed for elemental analysis at the coating and iron powder interfaces as well as particle size measurements before and after compaction of cross-sectioned powder compacts. The presence of aluminum, iron, oxygen, and carbon allowed for the determination of coating layer composition and thicknesses. Magnetic properties such as saturation magnetization and coercivity were measured on 3 mm diameter compacts using VSM from ± 5 T at 300K

in a Quantum Design PPMS. Saturation magnetization was determined by plotting the inverse magnetic field (1/Oe) vs. the magnetic moment per mass (emu/g) and analyzing the potential y-intercept relative to the highest magnetization measured. Elastic modulus and hardness were studied via an MTS nanoindenter, where measurements were taken within iron regions of powder compacts, 200 nm below the polished surface.

RESULTS

The above-mentioned methods successfully investigated magnetic, mechanical, and structural properties of alumina and magnetite coated iron powders and compacts. Mechanically milled iron powders became coated with Al_2O_3 when milled at room temperature with alumina media balls in an alumina vial. Iron powders milled with hardened steel media balls in an alumina vial also became coated with alumina. A dual layer of magnetite and alumina was developed with the addition of Fe_3O_4 sub-micron particles. Powder surfaces analyzed by SEM showed large amounts of texture and particle agglomerations, strong indication of a dense coating. XRD patterns of milled powders exposed alumina peaks for powders milled 4 h or longer in an alumina vial. Diffraction patterns also exemplified large regions of peak broadening and decreased peak intensity for longer milling times, evidence of internal defects and stressed regions [27].

SEM/EDS maps of powder compacts allowed for the elemental analysis of the coating material and metallic powders. Figure 2 exemplifies a powder compact from alumina and magnetite coated iron powders produced from the above-illustrated technique in Figure 1. Iron powders were first milled with hardened steel media balls in an alumina vial for 4 h and then milled for 1 h with Fe_3O_4 powder after the media balls were removed. Samples were then compacted and cured for 1 h at 700°C. Interfaces between iron powders were essentially aluminum-oxide and iron-oxide material, and most reasonably alumina from the milling media and magnetite from the added powder. Possible phase transformations to $FeAl_2O_4$ or Fe_2O_3 may have occurred [28, 29], but were undetectable via SEM. Alumina and magnetite content completely isolated iron powders from one another, therefore metal-on-metal contact points were eliminated. Additionally, studies utilized alumina and magnetite coatings separately. Preliminary EDS maps for both studies are seen in Figure 3, which illustrate iron powders coated with thick Al_2O_3 layers or very thin Fe_3O_4 layers. The thin magnetite thickness is most notable due to an insufficient amount of material added or the diffusion of Fe_3O_4 into Fe under reducing atmospheres.

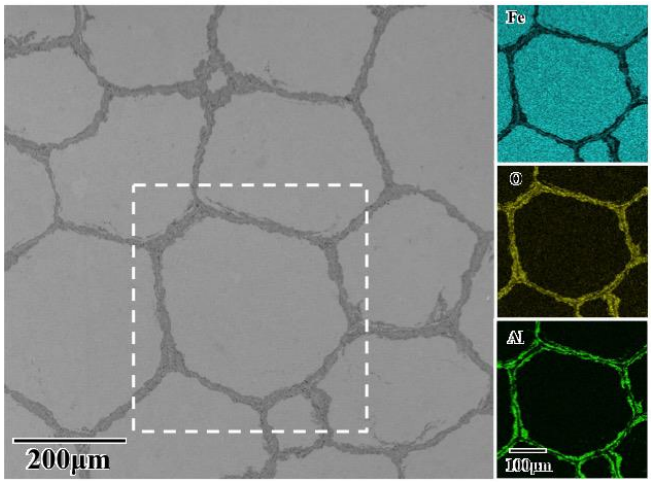

Figure 2. SEM image and respective EDS maps for a powder compact of Al_2O_3/Fe_3O_4 coated iron.

The highest saturation magnetization was measured for powder compacts with Fe_3O_4 coatings, as expected due to magnetite's ferrimagnetic nature and the large amount of iron content per volume. Lower magnetization results were found for powders milled for longer periods of time, which produced more internal defects and allowed for more alumina coating, when Al_2O_3 media was present. VSM results are seen in Figure 4a for powder compacts of Al_2O_3 coatings [27] and Al_2O_3/Fe_3O_4 dual coating layers. All powder compacts measured in this study had relatively low coercivities of 40 Oe or below.

Elastic modulus and hardness ratings were explored using nanoindentation at a depth of 200 nm. Results for powder compacts with Al_2O_3/Fe_3O_4 coated iron are presented in Figure 4b. As to be expected, elastic modulus remained constant; however, unexpectedly hardness decreased with increased amounts of milling. Higher curing temperatures resulted in lower hardness ratings, indication of proper stress relief and

recovery of iron. Mechanical properties of alumina coated iron powder compacts followed expected trends of increased hardness as more deformation was introduced [27]. Magnetite coated compacts have not been measured to date. Ideally, elastic modulus ratings would remain above 200 GPa and hardness above 3.5 GPa for strong mechanical structures.

CONCLUSIONS AND FUTURE WORK

We presented studies on Al_2O_3 and Fe_3O_4 coated iron powders by means of mechanical milling with relatively small media ball sizes. The magnetic and mechanical properties examined show promising features for use as SMCs in high frequency applications. Alumina coated powders produced from low-energy ball milling methods allowed for complete isolation of iron particles, eliminating metal-on-metal contact points. Although alumina is nonmagnetic, powder compacts still possessed relatively high saturation magnetization and low coercivities, as well as good elastic moduli and hardness ratings. Utilizing magnetite particles in place of alumina, greatly improved saturation magnetization; however, was less capable of isolating iron powders, due to possible diffusion between the iron/iron-oxide materials or insufficient amounts. Combining alumina and magnetite coatings proved to be detrimental to the magnetization results due to possible antiferromagnetic layers being formed.

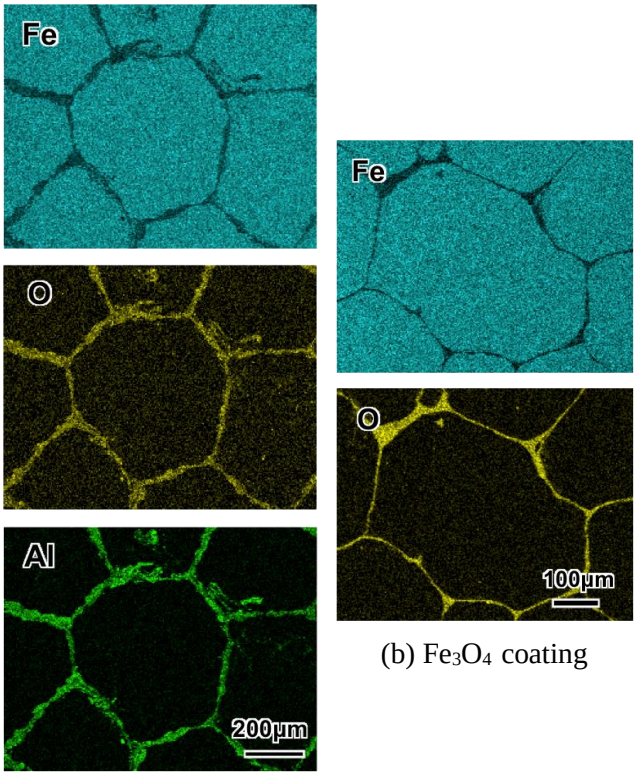

(a) Al_2O_3 coating

(b) Fe_3O_4 coating

Figure 3. SEM/EDS maps of polished powder compacts.

Future work will seek to optimize the alumina and magnetite coating layers, separately, for improved magnetization and mechanical properties. With proper isolation of ferrous powders, eddy current losses will be greatly reduced. The curing atmosphere used for the alumina coated powders was selected to reduce iron oxide content; however, this was undesirable for magnetite studies, therefore a pure argon atmosphere will be applied in future studies. Possible additions of alumina nanoparticles and higher curing temperatures will be utilized for improved bonding at the interfaces and potentially lower milling times required to produce a dense insulative coating. Additional amounts of magnetite material will be added to increase the insulation layer thickness and reduce eddy current flow when utilizing hardened steel media. Magnetic toroid samples will be produced to test AC and DC responses to measure eddy current and core losses of powder compacts. Non-contact resistivity measurements will be preformed to analyze the coating layers performance and the overall resistivity of the compacts. Mechanical testing bars will be produced to study the overall elastic modulus and hardness of the compacts rather than measuring individual powders within the compacts by means of nanoindentation.

Ideally, iron powders will be electrically insulated via a magnetic, resistive, high temperature coating material, so that eddy currents can be eliminated without hindering the soft magnetic properties of the SMC. Continuous research will study the optimization of structural, mechanical, electrical, and magnetic properties of coated ferrous powders for use as SMCs in high frequency applications.

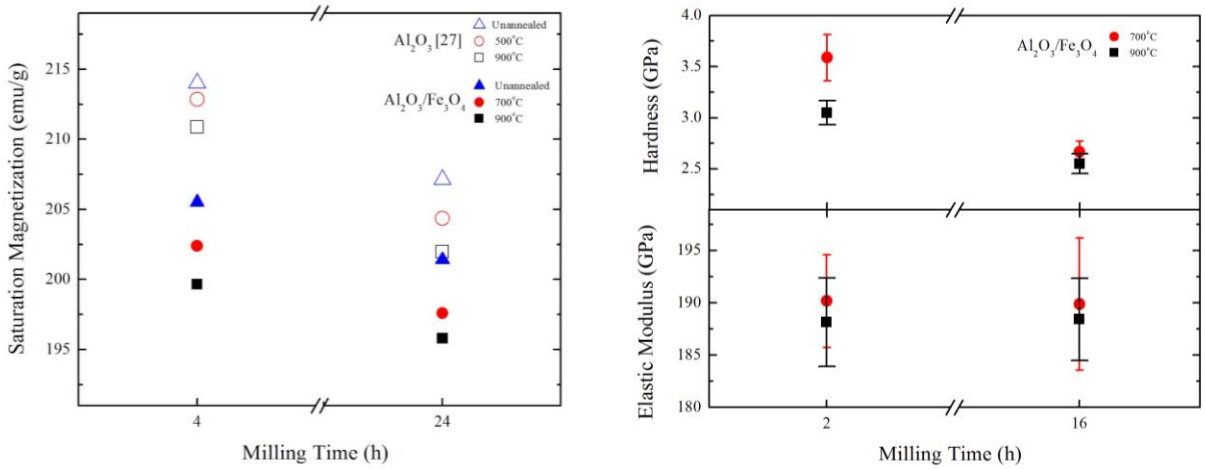

(a) Magnetization saturation results

(b) Nanoindentation results

Figure 4. Powder compacts with dual layers of Al_2O_3/Fe_3O_4 coated iron.

ACKNOWLEDGEMENTS

Authors KJS and MLT acknowledge funding from the National Science Foundation under Grant No. 235672. We thank Steve May for access to the vibrating sample magnetometer, Babak Anasori for nanoindentation measurements, and the Centralized Research Facilities for access to the x-ray diffractometer and scanning electron microscope at Drexel University.

REFERENCES

[1] Y.G. Guo et al. Australian Journal of Electrical and Electronics Engineering, 3(1), 2006.
[2] K. Ishii. Technical Report 55, Hitachi Chemical, May 2013.
[3] L.P. Lefebvre et al. Journal of Magnetism and Magnetic Materials, 176:L93–L96, 1997.
[4] A.H. Taghvaei et al. Journal of Magnetism and Magnetic Materials, 323:150–156, 2011.
[5] P. Gramatyka et al. Journal of Achievements in Materials and Manufacturing Engineering, 18(1-2), 2006.
[6] Y. Zhao et al. Advanced Materials, 17(7), April 2005.
[7] B.T. Kim. Journal of Electrical Engineering and Technology, 1(2):211–215, 2006.
[8] K. Janghorban H. Shokrollahi. Journal of Magnetism and Magnetic Materials, 317:61–67, April 2007.
[9] A.H. Taghvaei et al. Materials and Design, 30:3989–3995, 2009.
[10] N.B. Dhokey et al. Electronic Materials Letter, 10(3):591–596, 2014.
[11] Y.G. Guo et al. IEEE, 2002.
[12] H. Shokrollahi et al. Materials Chemistry and Physics, 114:588–594, 2009.
[13] H. Shokrollahi and K. Janghorban. Journal of Materials Processing Technology, 189:1–12, 2007.
[14] C. Cyr et al. IEEE Transactions on Magnetics, 45(3), March 2009.
[15] M. Streckova et al. Bulletin of Materials Science, 37(2):167–177, 2014.
[16] G. Uozumi et al. Materials Science Forum, 534-536:1361–1364, 2007.
[17] W. Liu et al. Surface and Coatings Technology, 200:5170–5174, 2006.

[18] A. Ozieblo K. Konopka. Materials Characterization, 46:125–129, 2001.
[19] Michel W. Barsoum. Fundamentals of Ceramics. Taylor Francis Group, 2003.
[20] J.M.D. Coey. Magnetism and Magnetic Materials. Cambridge, 2009.
[21] Q. Li et al. International Journal of Pharmaceutics, 280:77–93, 2004.
[22] H. Brunckov et al. Surface and Interface Analysis, 42:13–20, 2009.
[23] A.H. Taghvaei et al. Journal of Magnetism and Magnetic Materials, 322(23):3748–3754, 2010.
[24] Spex Equipment and Accessories.
[25] J.I. Langford. Journal of Applied Crystallography, 11, 1978.
[26] T.H. De Keijser et al. Journal of Applied Crystallography, 15, 1982.
[27] K.J. Sunday et al. In preparation, 2015.
[28] Y.L. Huang et al. Materials Science and Engineering A, 359:332–337, 2003.
[29] F. Jay et al. Journal of the American Ceramic Society, 89(11):3522–3528, 2006.